

Differentiating Histologic Malignancy of Primary Brain Tumors: Pentavalent Technetium-99m-DMSA

Tsuneo Hirano, Hidenori Otake, Takashi Shibasaki, Masaru Tamura and Keigo Endo

Department of Nuclear Medicine and Department of Neurosurgery, Gunma University, School of Medicine, Gunma, Japan

This study assessed pentavalent ^{99m}Tc -DMSA uptake in primary brain tumors and evaluated the relationship between retention and histologic malignancy. **Methods:** SPECT images of the brain were obtained at 30 min and 3 hr after intravenous administration of approximately 555 MBq ^{99m}Tc (V)-DMSA in patients with brain tumors. Sixty studies were performed in 57 patients and 63 lesions were demonstrated: 11 glioblastomas, 13 anaplastic astrocytomas (Grade 3), 11 astrocytomas (Grade 2), 18 meningiomas and 10 schwannomas. Uptake ratios, retention ratio and retention index were calculated and compared with tumor histology and malignancy grade. **Results:** Approximately 95% of both benign and malignant primary brain tumors were demonstrated by ^{99m}Tc (V)-DMSA SPECT images. False negative was noted in three cases. The early uptake ratios were closely related to the tumor vascularity but had no statistically significant difference in the tumor histology or histologic malignancy. The delayed uptake ratio, retention ratio and retention index were higher in the malignant tumors than the benign tumors. **Conclusion:** Technetium-99m(V)-DMSA washout from the tumor was highly dependent upon its histology and histologic malignancy. The delayed uptake ratio considerably reflected tumor histology and differentiated benign tumors from malignant tumors. The retention ratio and retention index significantly reflected tumor histology and histologic grade of primary brain tumors and clearly distinguished between benign and malignant tumors with statistically significant difference ($p < 0.05$). These results could suggest the clinical utility of ^{99m}Tc (V)-DMSA in imaging primary brain tumors and differentiating their histological malignancy grade noninvasively.

Key Words: pentavalent technetium-99m-DMSA; histologic malignancy; brain tumors; retention index; SPECT

J Nucl Med 1997; 38:20-26

CT and MRI can demonstrate smaller lesions due to their fine spatial resolution. Furthermore, their contrast enhancement, which is mainly dependent upon the disrupted blood-brain barrier, has been used to localize the tumors, but prediction of histopathological diagnosis is difficult. One of the most widely used radiopharmaceuticals, [^{201}Tc]chloride, has been reported to differentiate, to some extent, benign lesions from malignant lesions of the lung (1), thyroid gland (2) and brain tumors (3-7), depending upon the uptake ratio and prolonged washout phase of radiotracer from the tumor tissue (5-7).

Pentavalent ^{99m}Tc -dimercaptosuccinic acid (^{99m}Tc (V)-DMSA) was developed as a tumor imaging agent (8-9), and its accumulation has been reported in the medullary carcinoma of the thyroid (10), soft tissue tumors (11-12), lung cancers (13) and osseous metastatic tumors (13-14). We have established a simple and easy method to prepare ^{99m}Tc (V)-DMSA from commercially available DMSA kits (15) and have imaged primary brain tumors to assess clinical usefulness.

Watkinson et al. reported that there was no evidence of active uptake of ^{99m}Tc (V)-DMSA by squamous cell cancer, and the

tumor appeared to exhibit a prolonged washout phase of radioactivity when compared to the blood pool (16). We thought that there were several factors affecting tumor uptake, but only a prolonged washout phase may be hypothetically specific to tumor histology and histologic grade. Uptake ratios (early and delayed), retention ratio and retention index were calculated to evaluate and differentiate tumor-specific from nontumor-specific components. These numerical values were compared statistically with tumor histology and histologic grade of the primary brain tumors.

MATERIALS AND METHODS

Patients

Patients with a brain tumor on x-ray computed tomography (X-CT) or MRI were selected for this imaging. A [^{99m}Tc](V)-DMSA SPECT study was performed before surgical resection or stereotactic biopsy. Tumor size was measured by surgical specimen, contrast-enhanced CT and gadolinium-enhanced MR images. Tumor vascularity was also evaluated by dynamic SPECT images ([^{123}I]IMP or ^{99m}Tc -HMPAO), contrast-enhanced CT and gadolinium-enhanced MR image and classified into three groups: hypervascular, normovascular and hypovascular tumors.

Final diagnosis was made by histopathology of the specimens obtained by surgical procedure or stereotactic biopsy according to the WHO histological classification: glioblastoma, anaplastic astrocytoma (astrocytoma Grade 3), astrocytoma (astrocytoma Grade 2), pilocytic astrocytoma (astrocytoma Grade 1), meningioma and schwannoma.

Imaging

Technetium-99m(V)-DMSA was prepared using a commercially available dimercaptosuccinic acid (DMSA) kit. Briefly, the Techne® DMSA kit (Daiichi Radioisotope, Tokyo, Japan) contains 1.4 mg dimercaptosuccinic acid and 0.5 mg $\text{SnCl}_2 \cdot 2\text{H}_2\text{O}$. A DMSA kit added with 200 μl 7% of sodium bicarbonate solution (NaHCO_3) was reconstituted with 2 ml of ^{99m}Tc -pertechnetate solution (approximately 740 MBq) (15).

SPECT images of the brain were obtained at 30 min and 3 hr after intravenous administration of approximately 555 MBq ^{99m}Tc (V)-DMSA, using a ring-type SPECT scanner dedicated for brain studies (Headtome, Shimadzu Corp., Kyoto, Japan). Image acquisition was performed for approximately 0.4 to 0.7×10^6 counts per slice on 64×64 matrix with a 20% symmetric window at 140 keV. Butterworth and Ramachandran filters were used to reconstruct images in the transverse plane. Each image was corrected for tissue attenuation with the standard method using [^{99m}Tc]pertechnetate in a phantom. In-plane spatial resolution was 9.6 mm (FWHM).

Image Analysis

Technetium-99m(V)-DMSA SPECT images were compared with X-CT and MR images and tumor histology. Accumulation in the brain tumors was evaluated visually on SPECT images, and a

Received Oct. 18, 1995; revision accepted June 15, 1996.

For correspondence or reprints contact: Tsuneo Hirano, MD, Department of Nuclear Medicine, Gunma University, School of Medicine, 3-39-15 Showa-machi, Maebashi, Gunma 00371, Japan.

TABLE 1
Summary of 57 Patients with Primary Brain Tumors

Patient no.	Age (yr)	Sex	Histology	Location	Tumor size (cm)	Uptake ratio (Early/Delayed)	Retention (Ratio/Index)
1	45	M	Glioblastoma	Rt. basal ganglia	3.8 × 4.3 × 6.8	3.34/6.40	3.06/91.6
2	69	F	Glioblastoma	Rt. temporal lobe	3.5 × 4.0 × 4.7	3.91/9.46	5.55/142
3	47	M	Glioblastoma	Lt. temporal lobe	3.4 × 3.9 × 4.4	2.49/4.36	1.87/75.1
			Recurrence	Lt. temporal lobe	3.2 × 4.2 × 5.0	3.77/7.44	3.67/97.3
4	72	M	Glioblastoma	Frontal lobes	3.9 × 4.2 × 4.9	6.00/10.5	4.50/75.0
5	48	M	Glioblastoma	Lt. frontal lobe	4.0 × 4.3 × 5.6	4.79/9.43	4.64/96.9
6	10	F	Glioblastoma	Rt. temporal lobe	2.2 × 3.5 × 4.0	3.04/6.08	3.04/100
7	63	M	Glioblastoma	Rt. parietal lobe	2.8 × 3.8 × 4.6	3.62/7.80	4.18/115
8	42	F	Glioblastoma	Lt. temporo-parietal lobe	3.8 × 4.6 × 4.8	4.95/9.80	4.85/98.0
9	41	M	Glioblastoma	Lt. temporo-parietal lobe	4.4 × 4.5 × 5.8	5.63/12.9	7.27/129
10	77	M	Glioblastoma	Rt. temporal lobe	3.5 × 4.0 × 5.3	2.03/5.30	1.79/75.9
11	67	F	Astrocytoma (G 3)	Lt. Hippocampus	3.7 × 3.8 × 5.0	3.43/8.43	5.00/146
12	55	F	Astrocytoma (G 3)	Lt. fronto-parietal region	1.3 × 2.3 × 4.2	2.67/7.75	5.08/190
13	51	M	Astrocytoma (G 3)	Rt. temporal lobe	4.9 × 5.6 × 5.9	4.80/7.14	2.34/48.8
14	35	M	Astrocytoma (G 3)	Rt. frontal lobe	3.5 × 7.0 × 7.0	7.05/14.4	7.35/104
			Recurrence	Rt. frontal lobe	4.2 × 5.4 × 6.1	2.08/4.56	2.48/119
15	56	F	Astrocytoma (G 3)	Rt. temporal lobe	1.5 × 2.0 × 2.4	2.33/3.61	1.28/54.9
16	43	F	Glioma (G 3)	Basal ganglia	2.6 × 3.2 × 3.8	2.85/4.50	1.65/57.9
17	17	M	Astrocytoma (G 3)	Lt. thalamus	4.5 × 5.7 × 6.8	2.09/2.41	0.32/15.3
18	9	F	Anaplastic glioma	Hypothalamus	1.5 × 2.3 × 3.4	2.22/5.22	3.00/135
19	40	M	Astrocytoma (G 3)	Lt. parietal lobe	2.8 × 3.4 × 3.8	2.85/4.67	1.82/63.9
20	53	M	Astrocytoma (G 3)	Lt. frontal lobe	2.8 × 3.0 × 3.4	3.81/6.62	2.81/73.8
21	51	M	Astrocytoma (G 3)	Rt. frontal lobe	2.8 × 3.2 × 4.0	2.06/3.38	1.32/64.1
22	69	F	Astrocytoma (G 3)	Lt. temporo-parietal lobe	2.3 × 3.5 × 5.2	2.93/5.00	2.07/70.6
23	66	M	Recurrent astrocytoma (G 2)	Rt. fronto-parietal lobe	2.6 × 3.4 × 4.3	3.96/5.73	1.77/44.7
24	56	F	Astrocytoma (G 2)	Rt. temporal lobe	3.2 × 4.7 × 5.5	(-)/(-)	(-)/(-)
25	23	F	Astrocytoma (G 2)	Lt. temporo-parietal lobe	4.1 × 5.6 × 7.1	1.72/2.65	0.93/54.1
26	47	M	Astrocytoma (G 2)	Lt. cerebellum	3.9 × 4.5 × 4.6	2.28/3.90	1.62/71.1
27	48	F	Astrocytoma (G 2)	Lt. fronto-parietal lobe	2.6 × 4.2 × 4.3	2.76/3.16	0.40/14.5
28	67	F	Astrocytoma (G 2)	Rt. temporal lobe	3.0 × 3.4 × 3.8	2.72/3.62	0.90/33.1
29	68	F	Oligodendroglioma	Rt. frontal lobe	1.0 × 1.6 × 2.0	1.61/1.95	0.34/21.1
30	53	M	Oligoastrocytoma	Rt. frontal lobe	2.2 × 3.0 × 3.7	5.21/5.95	0.74/14.2
31	36	M	Recurrent glioma (G 2)	Rt. frontal lobe	3.0 × 4.9 × 5.6	5.31/7.69	2.38/44.8
32	49	M	Mixed oligoastrocytoma	Lt. temporal lobe	4.7 × 5.3 × 5.3	2.11/2.54	0.43/20.4
33	59	M	Mixed oligoastrocytoma	Lt. frontal lobe	2.0 × 2.4 × 3.0	(-)/(-)	(-)/(-)
34	22	M	Ganglioglioma	Lt. temporal lobe	1.2 × 1.6 × 2.6	2.12/3.05	0.93/43.9
35	30	M	Fibrillary astrocytoma	Lt. temporal lobe	4.1 × 5.3 × 6.4	(-)/(-)	(-)/(-)
36	36	M	Fibrillary astrocytoma	Lt. frontal lobe	3.6 × 4.2 × 4.6	3.86/4.28	0.42/10.9
37	45	M	Meningioma	Rt. F/T lobe	1.8 × 2.4 × 2.6	5.55/6.16	0.61/11.0
38	71	F	Meningioma	Torcular region	5.0 × 5.0 × 6.0	5.98/6.82	0.84/14.0
39	66	M	Meningioma	Falx	2.8 × 3.2 × 3.6	7.44/7.86	0.42/5.65
40	73	F	Meningioma	Plural lesions	1.4 × 2.1 × 2.3	2.71/2.89	0.18/6.64
			Meningioma	Plural lesions	2.8 × 3.1 × 3.8	2.56/2.48	-0.08/-3.13
			Meningioma	Plural lesions	0.7 × 1.0 × 1.5	2.08/2.29	0.21/10.1
41	48	M	Meningioma	Rt. parasagittal region	3.4 × 4.0 × 4.2	2.07/2.10	0.03/1.45
42	41	F	Meningioma	Lt. parietal lobe	2.4 × 2.8 × 3.6	2.01/2.36	0.35/17.4
43	67	F	Meningioma	Lt. sphenoid ridge	4.0 × 4.3 × 4.6	3.11/3.68	0.57/18.3
44	55	F	Meningioma	Plural lesions	5.6 × 6.6 × 7.0	2.82/3.38	0.56/19.9
			Meningioma	Plural lesions	1.7 × 2.0 × 2.3	2.11/2.50	0.39/18.5
			Meningioma	Plural lesions	1.0 × 1.3 × 1.9	2.20/2.11	-0.09/-4.19
			Meningioma	Plural lesions	2.4 × 2.6 × 2.8	1.96/2.72	0.76/38.8
45	47	M	Meningioma	Olfactory groove	3.6 × 4.2 × 6.0	4.67/6.00	1.33/28.5
46	37	M	Meningioma	Cavernous sinus	1.0 × 1.0 × 1.2	2.63/2.81	0.18/6.84
47	50	M	Recurrent meningioma	Lt. frontal region	2.0 × 3.0 × 3.4	2.67/2.82	0.15/5.62
48	57	F	Meningioma	Rt. temporal region	5.0 × 5.3 × 5.6	3.57/4.04	0.47/13.2
49	46	F	Meningioma	Lt. frontal region	3.4 × 3.8 × 4.2	6.51/6.56	0.05/0.77
50	51	M	Schwannoma	Lt. CP angle	1.0 × 1.2 × 1.3	3.35/3.71	0.36/10.7
51	53	M	Schwannoma	Rt. CP angle	3.0 × 3.2 × 4.8	5.05/5.11	0.06/1.19

Uptake ratio = maximum counts of the tumor over mean counts of the contralateral normal brain tissue on the early and delayed SPECT images; retention ratio = delayed uptake ratio - early uptake ratio; retention index = [(delayed uptake ratio - early uptake ratio)/early uptake ratio] × 100; (-) represents no tumor uptake.

TABLE 1
(Continued)

Patient no.	Age (yr)	Sex	Histology	Location	Tumor size (cm)	Uptake ratio (Early/Delayed)	Retention (Ratio/Index)
52	39	M	Schwannoma	Lt. CP angle	3.3 × 3.8 × 4.1	2.68/4.65	1.97/73.5
53	54	F	Schwannoma	Rt. CP angle	2.2 × 3.0 × 3.5	2.92/2.76	-0.16/-5.48
54	45	M	Schwannoma	Lt. CP angle	2.0 × 3.0 × 3.5	3.54/3.63	0.09/2.54
55	55	F	Schwannoma	Rt. CP angle	1.7 × 2.3 × 2.3	3.94/5.68	1.74/44.2
			Schwannoma	Lt. CP angle, plural lesions	2.3 × 2.7 × 4.3	3.86/5.10	1.24/32.1
56	53	F	Schwannoma	Lt. CP angle	2.8 × 2.9 × 3.3	2.20/2.87	0.67/30.5
57	40	F	Schwannoma	Rt. CP angle	3.5 × 4.1 × 6.0	3.11/4.50	1.39/44.7
			Recurrence		2.3 × 4.6 × 5.5	2.93/4.11	1.18/40.3

Uptake ratio = maximum counts of the tumor over mean counts of the contralateral normal brain tissue on the early and delayed SPECT images; retention ratio = delayed uptake ratio - early uptake ratio; Retention index = [(delayed uptake ratio - early uptake ratio)/early uptake ratio] × 100; (-) represents no tumor uptake.

circular ROI was drawn over the site of the greatest activity in the lesion (L). A homologous ROI was drawn over the contralateral normal brain tissue (N) of the similar location. Maximum and average counts were obtained, and uptake ratios, retention ratio and retention index were calculated on both early and delayed SPECT images (1).

Since a malignant tumor may often involve heterogeneous tissues such as highly malignant tissue, normal residual tissue, necrotic tissue and so on, and the most aggressive part of the tumor might be represented by the area of maximum counts, we decided to normalize the maximum counts of the tumor to the average counts of the normal brain tissue. Maximum counts in the contralateral normal region may not reflect true homologous tissue, therefore, we calculated uptake ratio (L/N) based on the maximum counts of the tumor normalized to the average counts of the homologous region (7, 13).

Two uptake ratios (early and delayed) and retention ratio (delayed uptake ratio - early uptake ratio) were obtained for each brain tumor. Retention index was calculated as: [(delayed uptake ratio - early uptake ratio)/early uptake ratio] × 100. Since we expected some difference in ^{99m}Tc(V)-DMSA uptake among the primary brain tumors, we compared uptake ratios, retention ratio and retention index with tumor histology and histologic grade using two-sided unpaired Student's t-test.

RESULTS

Table 1 presents results of the clinical findings, tumor histology, uptake ratios, retention ratio and retention index in all the patients examined. Sixty studies were performed in 57 patients and 63 lesions were positively demonstrated: 11 glioblastomas, 13 anaplastic astrocytomas (Grade 3), 11 astrocyto-

mas (Grade 2), 18 meningiomas, 10 schwannomas. There were 95.5% of the primary brain tumors demonstrated in this study. Three false-negative cases were observed in mixed oligoastrocytoma, fibrillary astrocytoma and astrocytoma (Grade 2). These cases were also negative on ²⁰¹TlCl and ¹⁸F-FDG studies. Five mixed astrocytomas were provisionally classified into astrocytoma (Grade 2) on this statistical analysis.

Hypervascular tumors were clearly demonstrated on both early and delayed images of ^{99m}Tc(V)-DMSA (Fig. 1). On the delayed images, glioblastomas and most of the astrocytomas (Grade 3) were more distinctly visible and showed significantly higher uptake ratios than on the early ones, but meningiomas and schwannomas showed similar or slightly higher uptake ratios than on the early ones. Therefore, calculated retention ratio and retention index were high in glioblastomas and astrocytomas (Grade 3) but low in meningiomas and schwannomas. Normo- or hypovascular tumors tended to show mildly or slightly increased uptake on the early images. Most of the astrocytomas (Grade 3) showed markedly increased uptake in comparison to the surrounding normal tissue on the delayed images, but astrocytomas (Grade 2) showed mildly increased uptake on the delayed images (Fig. 2). Therefore, calculated retention ratio and index were high in astrocytomas (Grade 3) and low in astrocytomas (Grade 2).

The early uptake ratio was not specific to the tumor histology (Fig. 3). The delayed uptake ratio (mean ± s.d., number of cases) (Fig. 4) would be very specific to the tumor histology and histological malignancy grade with statistically significant difference between glioblastoma (8.13 ± 2.54, 11) and astrocytomas (Grade 2) (4.05 ± 1.74, 11) (p < 0.003), glioblastomas

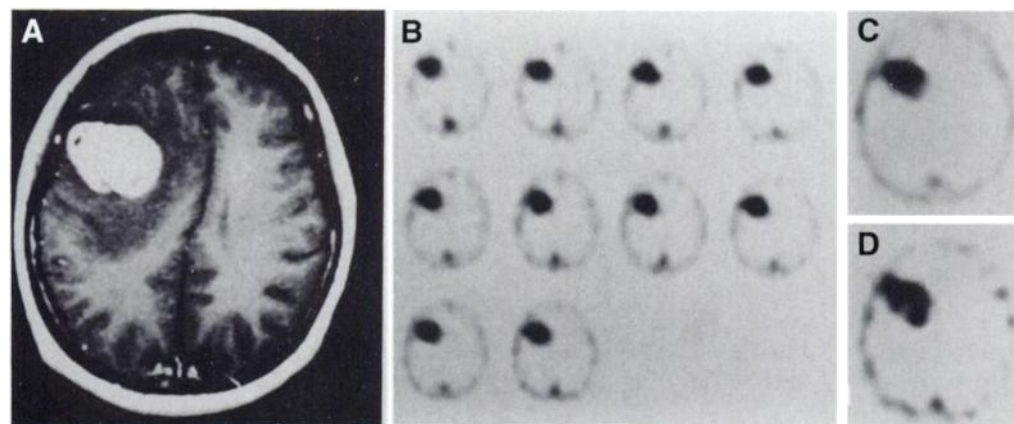


FIGURE 1. Glioblastoma. (A) Gd-enhanced MRI, (B) ^{99m}Tc(V)-DMSA dynamic, (C) early and (D) delayed static images. There is a large gadolinium-enhanced lesion in the left frontal lobe on MR (TR: 440 msec, TE: 15 msec) image. Technetium-99m(V)-DMSA dynamic images show an area of intense uptake in the left frontal lobe, indicative of a hypervascular lesion. There is an area of increased uptake on both early and delayed images with a high retention index of 96.9.

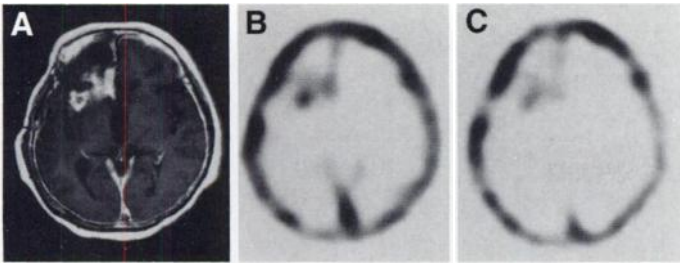


FIGURE 2. Astrocytoma (Grade 2). (A) Gd-enhanced MRI, (B) $^{99m}\text{Tc(V)}$ -DMSA early and (C) delayed static images. MR (TR: 500 msec, TE: 20 msec) image shows irregular enhancement with cystic components in the left frontal lobe. There is mildly increased uptake noted in the left frontal lobe on the early image and relatively decreased uptake on the delayed image, representing fast washout from the lesion. Calculated retention index was as low as 14.5.

and meningiomas (3.87 ± 1.90 , 18) ($p < 0.0001$), glioblastomas and schwannomas (4.21 ± 0.97 , 10) ($p < 0.0002$), astrocytomas (Grade 3) (5.98 ± 3.09 , 13) and meningiomas ($p < 0.025$), and astrocytomas (Grade 3) and schwannomas ($p < 0.098$). There was no significant statistical difference between glioblastomas and astrocytomas (Grade 3), astrocytomas (Grade 3) and astrocytomas (Grade 2), astrocytomas (Grade 3) and schwannomas, astrocytomas (Grade 2) and meningiomas, astrocytomas (Grade 2) and schwannomas or meningiomas and schwannomas.

The retention ratio (mean \pm s.d., n) was obtained by (delayed uptake ratio - early uptake ratio). There was significant statistical difference between glioblastomas (4.04 ± 1.61 , 11) and astrocytomas (Grade 2) (0.99 ± 0.67 , 11) ($p < 0.0001$), glioblastomas and meningiomas (0.39 ± 0.36 , 18) ($p < 0.0001$),

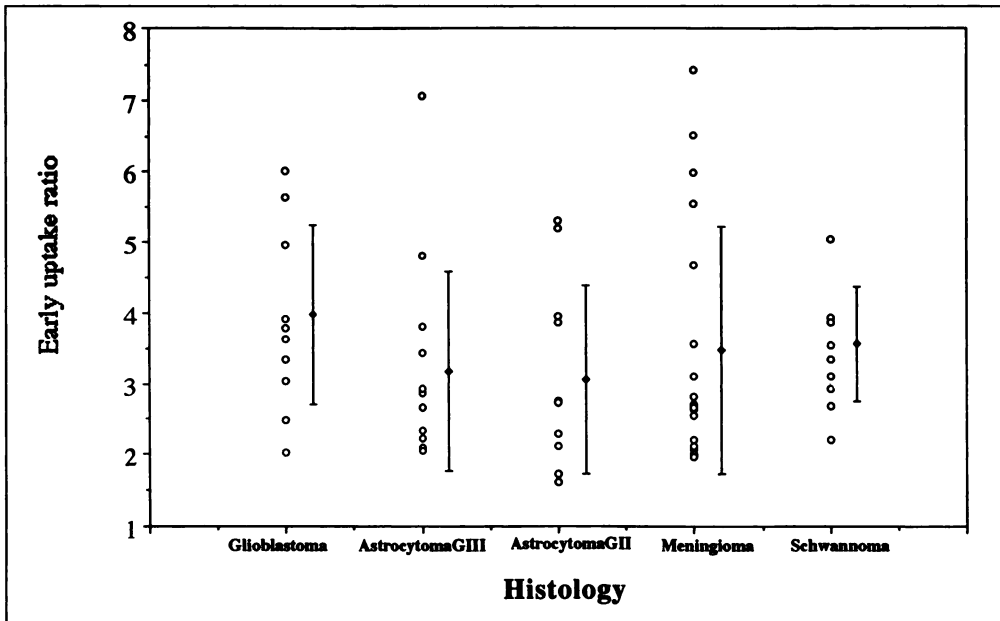


FIGURE 3. Early uptake ratio. There is no statistically significant difference.

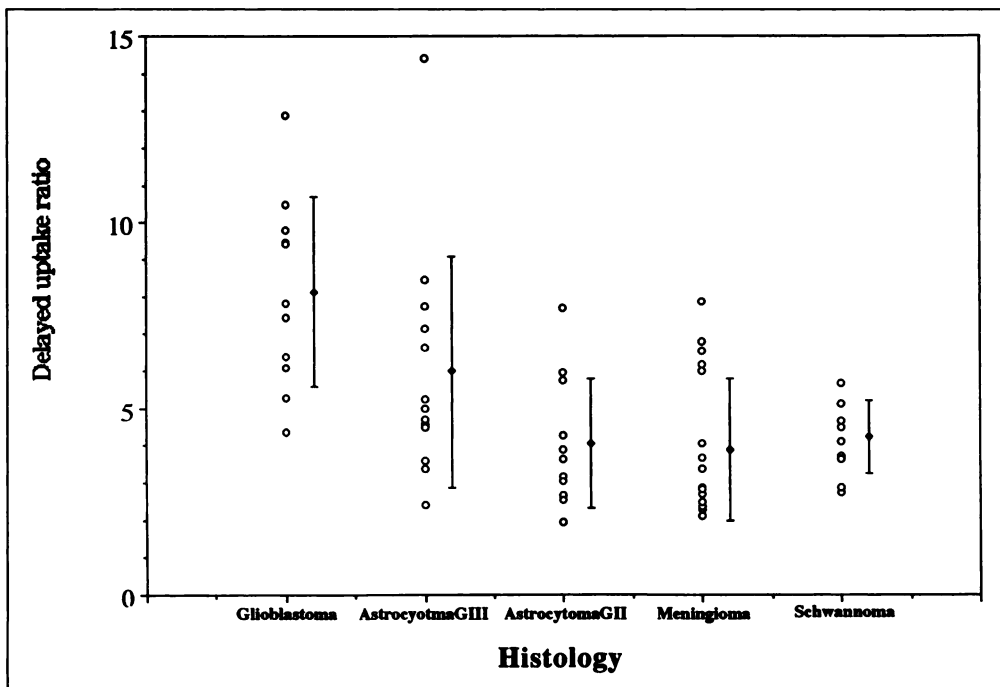


FIGURE 4. Delayed uptake ratio. There is some specific tendency to the tumor histology.

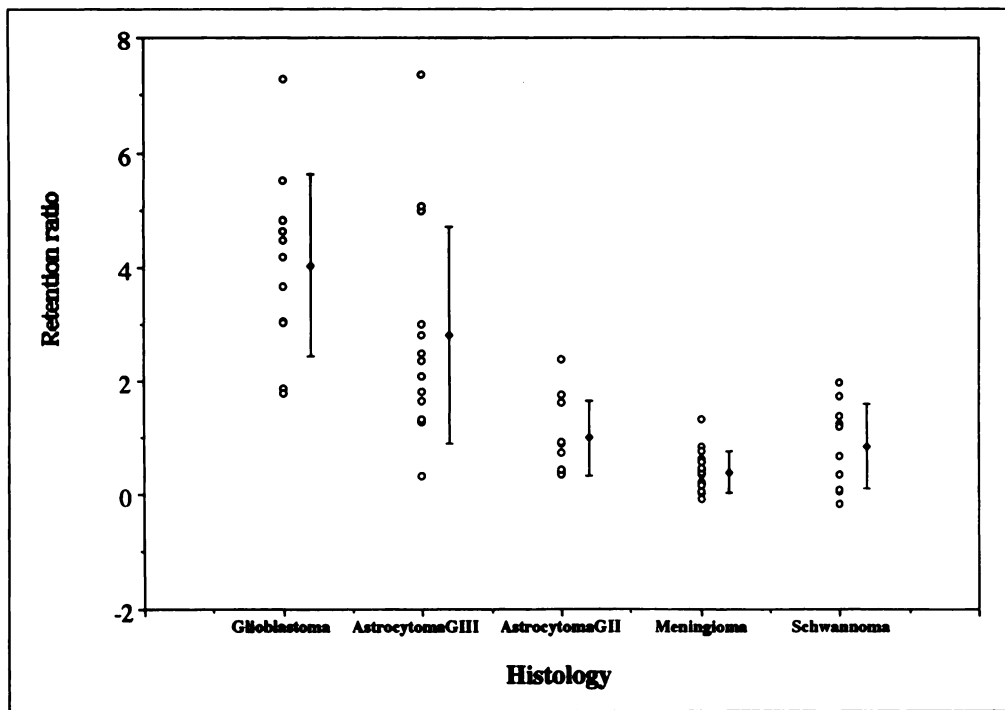


FIGURE 5. Retention ratio. There is a statistically significant difference between malignant tumors (glioblastoma and astrocytoma Grade 3) and benign tumors (astrocytoma Grade 2, meningioma and schwannoma).

glioblastomas and schwannomas ($0.85 \pm 0.75, 10$) ($p < 0.0001$), astrocytomas (Grade 3) ($2.81 \pm 1.93, 13$) and astrocytomas (Grade 2) ($p < 0.007$), astrocytomas (Grade 3) and meningiomas ($p < 0.0001$), astrocytomas (Grade 3) and schwannomas ($p < 0.007$), astrocytomas (Grade 2) and meningiomas ($p < 0.004$) and meningiomas and schwannomas ($p < 0.034$) but no significant statistical difference between glioblastomas and astrocytomas (Grade 3) or astrocytomas (Grade 2) and schwannomas (Fig. 5).

The retention index was calculated by (retention ratio/early uptake ratio) \times 100, then retention index also became specific to the tumor histology and histologic grade (Fig. 6). The retention index (mean \pm s.d., n) easily differentiated glioblastomas ($99.3 \pm 21.8, 11$) from benign astrocytomas ($33.9 \pm 19.4, 11$) (Grade 2) ($p < 0.0001$), meningiomas ($11.6 \pm 10.9,$

18) ($p < 0.0001$) and schwannomas ($27.4 \pm 24.9, 10$) ($p < 0.0001$), but there was no significant statistical difference between glioblastomas and astrocytomas (Grade 3). Astrocytomas (Grade 3) ($87.9 \pm 48.0, 13$) were differentiated from astrocytomas (Grade 2) ($p < 0.003$), meningiomas ($p < 0.0001$) and schwannomas ($p < 0.002$). Meningiomas and schwannomas were differentiated from each other ($p < 0.028$). Astrocytomas (Grade 2) were differentiated from meningiomas ($p < 0.0005$) but were not differentiated from schwannomas (Table 2). The retention index also showed significant statistical difference between malignant tumors (glioblastomas and astrocytomas (Grade 3) and benign tumors (astrocytomas (Grade 2), meningiomas and schwannomas) ($p < 0.0001$) but showed no significant statistical difference between glioblastomas and astrocytomas (Grade 3) or astrocytomas (Grade 2) and schwannomas.

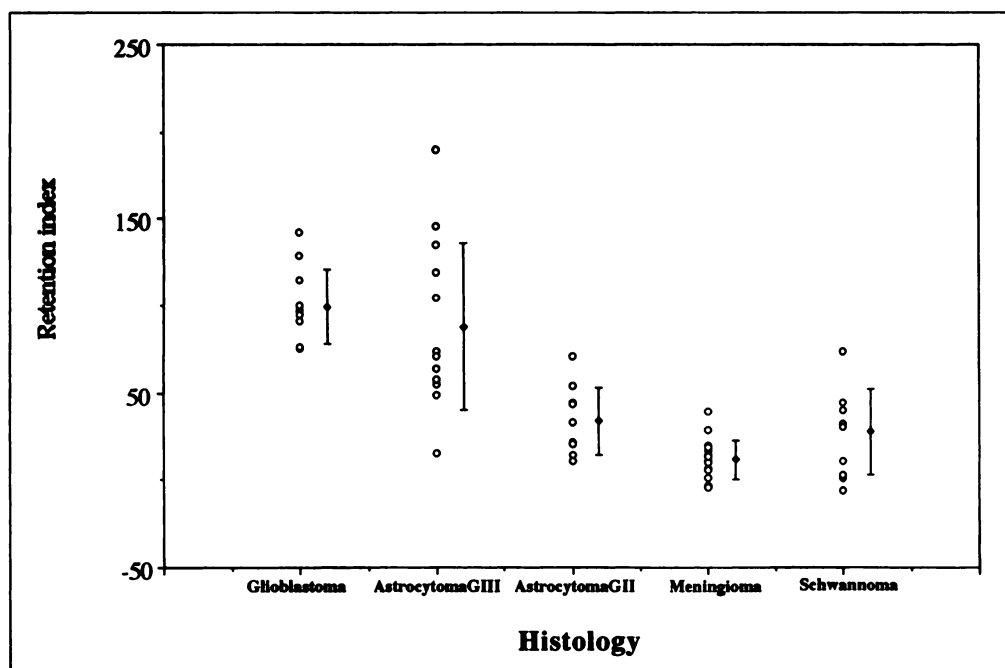


FIGURE 6. Retention index: There is a statistically significant difference between malignant tumors (glioblastoma and astrocytoma Grade 3) and benign tumors (astrocytoma Grade 2, meningioma and schwannoma).

TABLE 2
Uptake Ratios and Retention Index (mean \pm s.d.) of 63 Lesions

Histology	Number of lesions demonstrated	Early uptake ratio (Mean \pm s.d.)	Delayed uptake ratio (Mean \pm s.d.)	Retention ratio (Mean \pm s.d.)	Retention index (Mean \pm s.d.)
Glioblastoma	11	3.98 \pm 1.27	8.13 \pm 2.54	4.04 \pm 1.61	99.3 \pm 21.8
Astrocytoma (Grade 3)	13	3.17 \pm 1.41	5.98 \pm 3.09	2.81 \pm 1.93	87.9 \pm 48.0
Astrocytoma (Grade 2*)	11†	3.06 \pm 1.33	4.05 \pm 1.74	0.99 \pm 0.67	33.9 \pm 19.4
Meningioma	18	3.48 \pm 1.75	3.87 \pm 1.90	0.39 \pm 0.36	11.6 \pm 10.9
Schwannoma	10	3.56 \pm 0.80	4.21 \pm 0.97	0.85 \pm 0.75	27.4 \pm 24.9

*Five mixed gliomas were classified into astrocytoma Grade 2 for statistical analysis.

†Three negative cases were not included.

DISCUSSION

Although $^{99m}\text{Tc}(\text{V})\text{-DMSA}$ has been reported to accumulate in many kinds of tumors, such as soft tissue tumors, medullary carcinoma of the thyroid and lung cancers, the exact mechanism of tumor accumulation has not been identified yet.

Technetium-99m(V)-DMSA could not penetrate the intact blood-brain barrier and did not accumulate in the normal brain tissue or choroid plexus of the cerebral ventricle. There was normal accumulation noted in the scalp, orbital tissue and pituitary gland. Blood-pool activity was also seen in the venous sinuses, however, abnormal accumulation could be identified easily against low background activity of the normal brain tissue.

Technetium-99m(V)-DMSA SPECT demonstrated both benign and malignant brain tumors with high sensitivity of above 95%. Hypervascular tumors tended to show increased uptake and could be well-identified on the early images, but hypovascular tumors, such as astrocytomas (Grade 2), showed mildly or slightly increased uptake on the early images. On the delayed images, the uptake became relatively high in malignant tumors and the same or slightly higher in benign tumors in contrast to the surrounding normal brain tissue. Therefore, detectability of this study tended to be high in hypervascular and malignant tumors but low in hypovascular and benign tumors, such as astrocytomas (Grade 2), which likely results in false negatives.

The early uptake ratio did not show a specific tendency to the tumor histology (Fig. 3) and might reflect a combination of several factors affecting tumor accumulation, such as tumor vascularity, tissue permeability, metabolic activity and disrupted blood-brain barrier. Malignant tumors tended to show an increased uptake in contrast to the surrounding normal brain tissue on delayed images, and the delayed uptake ratio became relatively higher (Fig. 4). Therefore, the delayed uptake ratio would seem to depend mainly upon the tumor retention of radiotracer and less upon the factors affecting the early uptake ratio as time passed. This could solely reflect a prolonged washout phase specific to the tumor histology. These findings clinically substantiated the Watkinson's report that there was no active tumor uptake and the tumors appeared to exhibit a prolonged washout phase (16).

The retention ratio was more specific to the tumor histology due to subtracting nontumor-specific components (Fig. 5). There was significant statistical difference between glioblastomas and astrocytomas (Grade 2) ($p < 0.0012$), glioblastomas and meningiomas ($p < 0.0001$), glioblastomas and schwannomas ($p < 0.0001$), astrocytomas (Grade 3) and astrocytomas (Grade 2) ($p < 0.027$), astrocytomas (Grade 3) and meningiomas ($p < 0.0001$), astrocytomas (Grade 3) and schwannomas

($p < 0.0025$), astrocytomas (Grade 2) and meningiomas ($p < 0.005$) and meningiomas and schwannomas ($p < 0.034$), but there was no significant statistical difference between glioblastomas and astrocytomas (Grade 3) or astrocytomas (Grade 2) and schwannomas.

The retention index was calculated by (retention ratio/early uptake ratio) \times 100 to further reduce the nonspecific effect, then the retention index became more specific to the tumor histology and histologic grade (Fig. 6). The retention index could easily differentiate glioblastomas from benign astrocytomas (Grade 2) ($p < 0.0004$), meningiomas ($p < 0.0001$) and schwannomas ($p < 0.0001$), but there was no significant statistical difference between glioblastomas and astrocytomas (Grade 3). Astrocytomas (Grade 3) could be differentiated from astrocytomas (Grade 2) ($p < 0.0098$), meningiomas ($p < 0.0001$) and schwannomas ($p < 0.0001$). Meningiomas and schwannomas could be differentiated from each other ($p < 0.028$). Astrocytomas (Grade 2) were differentiated from meningiomas ($p < 0.0038$) but were not differentiated from schwannomas.

Watkinson et al. reported in their animal tumor model that there was no evidence of active uptake of $^{99m}\text{Tc}(\text{V})\text{-DMSA}$ by squamous cell cancer, and the tumors appeared to exhibit a prolonged washout phase of radioactivity when compared to the blood pool (16). We thought that there were several factors affecting tumor uptake, such as vascularity, permeability, metabolic activity and cell proliferation.

The early uptake ratio could be modified by the various factors not specific to the tumor histology or histologic grade. The delayed uptake ratio had a specific tendency according to the tumor histology but less specific than the retention ratio and index because of some modification by the various factors composing the early uptake ratio. Both retention ratio and retention index was very specific to and could clearly differentiate between the tumor histology and histologic grade of the primary brain tumors. These differentiations would solely depend upon the prolonged washout phase, which was very specific to the tumor malignancy and histologic grade.

Technetium-99m(V)-DMSA could be easily available and clearly demonstrate primary brain tumors with sensitivity above 95%. Tumor malignancy grade could also be predicted noninvasively by numerical scores, which would be very useful to determine therapeutic methods. Three geometric isomers have been reported to coexist in the $^{99m}\text{Tc}(\text{V})\text{-DMSA}$ preparations (8), and the question as to which constituents are specific to the tumors still remains. The tumor uptake was mainly dependent upon its vascularity, but the retention was solely dependent upon the tumor histology and histologic malignancy. The exact

mechanism of the tumor uptake has been investigated but not identified clearly yet. Further basic and clinical investigation is necessary to understand the behavior of this promising radio-pharmaceutical.

REFERENCES

1. Tonami N, Shuke N, Yokoyama K, et al. Thallium-201 SPECT in the evaluation of suspected lung cancer. *J Nucl Med* 1989;30:997-1004.
2. Tonami N, Hisada K. Clinical experience of tumor imaging with ²⁰¹Tl-chloride. *Clin Nucl Med* 1977;2:75-81.
3. Kaplan WD, Takvorian T, Morris JH, Rumbaugh CL, Connolly BT, Atkins HL. Thallium-201 brain tumor imaging: a comparative study with pathologic correlation. *J Nucl Med* 1987;28:47-52.
4. Ancrì D, Bassett JY, Lonchampt MF, et al. Diagnosis of cerebral lesions by ²⁰¹Tl. *J Nucl Med* 1978;128:417-422.
5. Black KL, Hawkins RA, Kim KT, Becker DP, Lerner C, Marciano D. Use of ²⁰¹Tl SPECT to quantitate malignancy grade of gliomas. *J Neurosurg* 1989;71:342-346.
6. Mountz JM, Stafford-Schuck K, McKeever PE, Taren J, Beierwaltes WH. Thallium-201 tumor/cardiac ratio estimation of residual astrocytoma. *J Neurosurg* 1988;68:705-709.
7. Kim KT, Black KL, Marciano D, et al. Thallium-201 SPECT images of brain tumors: methods and results. *J Nucl Med* 1990;31:965-969.
8. Westera G, Gadze A, Horst W. A convenient method for the preparation of ^{99m}Tc(V)-dimercaptosuccinic acid (^{99m}Tc(V)-DMSA). *Int J Appl Radiat Isot* 1985;36:311-312.
9. Blower PJ, Singh J, Clarke SEM. The chemical identity of pentavalent ^{99m}Tc-dimercaptosuccinic acid. *J Nucl Med* 1991;32:845-849.
10. Ohta H, Yamamoto K, Endo K, et al. A new imaging agent for medullary carcinoma of the thyroid. *J Nucl Med* 1984;25:323-325.
11. Ohta H, Endo K, Fujita T, et al. Imaging of soft tissue tumors with ^{99m}Tc(V)-dimercaptosuccinic acid, a new tumor seeking agent. *Clin Nucl Med* 1984;9:568-573.
12. Ohta H, Endo K, Fujita T, Konishi J, Torizuka K, Horiuchi K, Yokoyama A. Clinical evaluation of tumor imaging using ^{99m}Tc(V)-dimercaptosuccinic acid, a new tumor seeking agent. *Nucl Med Commun* 1988;9:105-116.
13. Hirano T, Otake H, Yoshida I, Endo K. Primary lung cancer SPECT imaging with pentavalent ^{99m}Tc-DMSA. *J Nucl Med* 1995;36:202-207.
14. Lamki L, Shearer R. Technetium-99m-DMSA uptake by metastatic carcinoma of the prostate. *J Nucl Med* 1985;25:733-734.
15. Hirano T, Tomiyoshi K, Ying Jian Zhang, Ishida T, Inoue T, Endo K. Preparation and clinical evaluation of ^{99m}Tc-DMSA for tumor scintigraphy. *Eur J Nucl Med* 1994;21:82-85.
16. Watkinson JC, Allen SJ, Laws DE, Lazarus CR, Maisey MN, Clarke SEM. The pharmacokinetics and biodistribution of ^{99m}Tc(V)-dimercaptosuccinic acid in an animal tumor model. *J Nucl Med* 1992;32:1235-1238.

Fasting Improves Discrimination of Grade 1 and Atypical or Malignant Meningioma in FDG-PET

Uwe Cremerius, Roland Bares, Joachim Weis, Osama Sabri, Michael Mull, J. Michael Schröder, Joachim M. Gilsbach and Udalrich Buell

Departments of Nuclear Medicine, Neuropathology, Neuroradiology and Neurosurgery, Aachen University of Technology, Germany

We investigated the use of PET with 2[¹⁸F]fluoro-2-deoxy-D-glucose (FDG) to discriminate between atypical or malignant and grade 1 meningiomas. The influence of fasting state and high-dose corticosteroid medication was analyzed retrospectively. **Methods:** Preoperative PET scans of 75 patients with suspected diagnosis of intracranial meningioma were evaluated using standardized uptake values (SUV) and tumor-to-contralateral gray matter ratios (TGR) of FDG uptake. Fifty-one of 75 patients fasted before the PET scan, and 27 of 75 patients were studied under high-dose corticosteroid medication. Eighteen tumors had recurred. PET results were compared to histopathological grading. **Results:** PET correctly identified 8/9 atypical or malignant meningiomas and 58/66 grade 1 meningiomas using TGR and a threshold of 1.05 in primary meningioma and 0.85 in tumor recurrence. This corresponds to a specificity of 0.88 for the detection of higher tumor grading. Specificity was significantly higher in fasting compared to nonfasting subjects (0.96 versus 0.73; $p < 0.025$). SUV quantification lead to a reduced specificity of 0.77 at the same level of sensitivity. The only false-negative PET finding occurred in a recurrent meningioma, which had been operated on four times before. **Conclusion:** Overnight fasting before injection is needed to improve the diagnostic accuracy of FDG-PET for noninvasive metabolic grading of meningioma. Hyperglycemia in nonfasting patients and in diabetic patients may lead to overestimation of meningioma grading.

Key Words: meningioma; grading; PET; fluorine-18-FDG

J Nucl Med 1997; 38:26-30

Meningiomas are the most common benign intracranial tumors. They represent about 15% of all primary intracranial tumors. Meningiomas are not always curable. The rate of recurrence depends on the completeness of removal, the site of

the tumor and its biological aggressiveness (1). In a large series, recurrences were found in 7% of grade 1 meningiomas, in 35% of grade 2 and 70% of grade 3 tumors (2). Glucose consumption of intracranial meningioma assessed by PET using 2[¹⁸F]fluoro-2-deoxy-D-glucose (FDG) has been proposed as an index of tumor aggressivity and probability of recurrence by Di Chiro et al. (3).

Recent studies have been published that addressed the effect of blood glucose levels on FDG uptake in cancer (4,5). Little, however, is known about the influence of metabolic factors on FDG uptake in intracranial tumors and brain tissue. Various investigators have stressed the importance of the fasting state for PET scans using FDG in oncology (4,6). It is not known whether patients in PET studies related to neuro-oncology should also fast before the scan. Additionally, the effect of medication, which may influence glucose metabolism, has not yet been systematically studied. A large number of meningioma patients preoperatively receive high-dose corticosteroids to reduce peritumoral edema. Corticosteroids are known to stimulate gluconeogenesis in hepatic tissue (7) and may thus have an effect on FDG uptake similar to nutritive glucose.

The aim of this study was to evaluate the use of FDG-PET as a noninvasive metabolic assessment of intracranial meningiomas compared to histopathological grading. We also analyzed the influence of fasting state, high-dose corticosteroid medication and previous surgical treatment.

METHODS

Patients

Seventy-five patients (51 women, 24 men; mean age 58 yr; range 14-81 yr) with the neuroradiological diagnosis of suspected meningioma were examined by FDG-PET within 21 days before neurosurgery. Informed consent was obtained from all patients. The diagnosis was proven histologically in all patients. According

Received Nov. 29, 1995; revision accepted May 29, 1996.
For correspondence or reprints contact: Uwe Cremerius, MD, Department of Nuclear Medicine, RWTH Aachen, Pauwelsstr. 30, D-52057 Aachen, Germany.